AN OVERVIEW OF TRENDS AND REGIONAL DISTRIBUTION OF THERMAL ICE LOADS ON DAMS IN NORWAY*

Chris PETRICH, Bård ARNTSEN
Research Directors
NORTHERN RESEARCH INSTITUTE NARVIK, NARVIK

NORWAY

SUMMARY

Norway is a mountainous hydropower nation that spans a wide range of climatic conditions. Ice contributes significantly to the design load of dams common in Norway. This study presents a first evaluation of expected regional differences of thermal static ice loads in hydropower reservoirs applied to Norway. Regionally interpolated air temperatures of the past 60 years were used to drive a thermo-dynamic model of ice growth and melt. Derived ice thickness and temperatures were converted into stresses from which line loads on a hypothetical vertical dam face were calculated. The study focusses on temporal development and regional distribution of seasonally maximum line loads. Model results are consistent with the small body of suitable field measurements in Norway. Additional measurements in reservoirs with thermal ice loads above 100 kN/m would be desirable for model validation. Based on model results, seasonal maximum line loads tend to be higher in colder regions. However, regional differences were found to be significant and not always trivially predicted. While the long-term trend is toward lower ice loads, trends differ regionally with some mountainous regions showing no long-term change. Even though inter-annual variability was found to be high, some locations have lowered ice loads significantly during the past 60 years, well in excess of their inter-annual variability. The model is transferable to other

---

* *Synthèse des tendances et répartition régionale des charges thermiques de glace sur les barrages norvégiens*

geographic regions and can help identify locations that may see ice loads consistently lower than currently assumed, and provide long-term context for ice load measurements. This may affect the selection of dam design, and the choice of rehabilitation methods during safety reviews.

Keywords: ice pressure, climate, dam failure, safety of dams, design, reinforcement, gravity dam.

RÉSUMÉ

La Norvège est une nation d'hydroélectricité en montagne, avec une large plage de conditions climatiques. La charge de projet des barrages comprend souvent une contribution significative de la glace. Cette étude présente une première évaluation des différences régionales attendues des charges de glace statiques thermales dans les réservoirs hydroélectriques en Norvège. Des températures de l'air interpolées régionalement pour les 60 dernières années ont été utilisées pour piloter un modèle thermodynamique de croissance et fonte de la glace. L'épaisseur et la température dérivées pour la glace ont été converties en contraintes dont les charges linéaires ont été calculées sur une paroi de barrage verticale hypothétique. Cette étude se concentre sur le développement temporel et la distribution régionale des charges linéaires maximales par saison. Les résultats du modèle sont cohérents avec le petit corpus de mesures sur site adéquates en Norvège. Des mesures supplémentaires dans les réservoirs avec des charges thermiques de glace supérieures à 100 kN/m seraient nécessaires pour la validation du modèle. Sur la base des résultats du modèle, les charges linéaires maximales saisonnières tendent à être supérieures dans les régions froides. Toutefois, des différences régionales notoires ont été identifiées, et par toujours prévisibles de manière simple. Alors qu'il existe une tendance à long terme vers des charges de glace inférieures, les tendances diffèrent régionalement avec certaines régions montagneuses ne montrant pas d'évolution à long terme. Même si la variabilité interannuelle est élevée, la charge de glace a diminué de manière significative à certains emplacements au cours des 60 dernières années, bien au delà de la variabilité inter-annuelle. Le modèle est transférable à d'autres régions géographiques et peut aider à identifier les zones pouvant présenter des charges bien plus basses que supposées actuellement, et fournir un contexte à long terme pour les mesures des charges de glace. Cela pourra affecter la sélection des modèles de barrages, et le choix des méthodes de réhabilitation pendant les revues de sécurité.

1.   INTRODUCTION

Norway has over 3000 dams, over half of which are concrete dams [1]. Static ice loads are considered as part of dam design and during period safety review. They present a significant fraction of the total design load of dams of low height (<15 m) common in Norway [1]. Ice loads are traditionally considered driven by the thermal expansion of ice, although measurements showed that slow water level fluctuations covering a range similar to ice thickness have the potential to cause loads of similar magnitude [2]. Commonly used static ice loads in dam design include 100 to 150 kN/m in Norway, regionally-dependent 50 to 200 kN/m in Sweden, ice thickness-dependent 150 to 220 kN/m in Canada, and at least up to 300 kN/m in Russia [3]. While the climate in Norway ranges from temperate to polar, no specific rules are in place to help select design ice loads based on regional differences. Instead, climatic conditions may be considered on a case-by-case basis. To-date, no global failures of dams due to ice loads have been reported in Norway [1], raising the question whether current design practices are too conservative.

The intent of this study is to assess on theoretical grounds whether regional differences in thermal ice loads should be expected to be significant in Norway. The presence of significant differences would motivate a closer look into ice load magnitudes both at the theoretical level and through field measurements. In addition, rates of change and corresponding regional differences were to be assessed given a generally observed warming trend.

The focus of this study is on trends and regional differences rather than on actual magnitudes in any particular reservoir. This allowed for simplifying assumptions to be made on reservoir geometry and local environmental conditions. Based on those assumptions established methods could be used to model ice growth. However, there is no universally accepted, practical model of static thermal ice loads on dams [4]. This study follows an approach based on a non-linear rheology that has repeatedly been found to be successful in explaining ice stress measurements over the period of weeks to months, including in Norway [5,6,7].

2.   METHODS

Ice loads in reservoirs were modeled as follows: a record of air temperature was used to drive an ice growth model. The model produced a record of the development of ice thickness, and of temperatures at various depths in the ice. At each depth, ice temperature changes were used to calculate thermal stresses, and the resulting vertical stress profile was integrated over the thickness of the ice to determine the line load against a vertical dam.

The data source used for this study is the seNorge 2 gridded two-meter air temperature dataset for mainland Norway [8]. The dataset was developed for use in climatological and hydrological applications with grid spacing appropriate to resolve the Norwegian drainage network. Daily average temperatures are provided on a 1 km grid back to 1957. The data are based on interpolation of observational data in the MET Norway's Climate Databases (KDVH) and are regarded as an unbiased estimate for air temperatures above -30 °C. At temperatures below -30 °C, interpolated air temperatures have been found to show a systematic warm bias [8].

Air temperature data from 1957 through 2016 were extracted at the locations of 1709 hydropower reservoirs listed in the lake database of the Norwegian Water Resources and Energy Directorate (NVE). While the density of the reservoirs is not homogeneous across the country, the selection ensures that the results of this study are relevant for the most typical production areas in Norway.

The ice growth model is a one-dimensional heat transfer model (a column model) that treats phase change based on the enthalpy–porosity approach [9]. The energy conservation equation solved is

$$\overline{c\rho}\frac{dT}{dt} = \frac{d}{dz}\overline{k}\frac{d^2T}{dz^2} - L\rho\frac{d\varphi}{dt} + S \tag{1}$$

where S is the source term at the boundaries of the numerical domain, t is time, z is distance along the vertical axis, $L=334\times10^3$ J/kg K is the latent heat of fusion of ice, $\rho=920$ kg/m^3 is the density of ice, φ is the local liquid volume fraction (i.e., within a numerical grid cell), T is the local temperature of ice or water (i.e., within a numerical grid cell), and the thermodynamic properties of the ice within each grid cell are

$$\overline{c\rho} = c_w\rho_w\varphi + c_i\rho_i(1-\varphi) \tag{2}$$

where c_w = 4200 J/kg K and c_i =2100 J/kg K is the specific heat capacity of water and ice, respectively, and ρ_w=1000 kg/m^3 and ρ_i=920 kg/m^3 is the density of water and ice, respectively, and

$$\overline{k} = k_w\varphi + k_i(1-\varphi) \tag{3}$$

where k_w =0.56 W/m K and k_i =2.0 W/m K are the thermal conductivity of water and ice, respectively. However, as long as no ice is present, wind-driven turbulent mixing is assumed with an effective k_w=400 W/kg m (cf. [10] for order of magnitude). In cells that are neither completely solid nor completely liquid, i.e. $0<\varphi<1$, the liquid phase φ is iteratively adjusted to maintain $T=0$ °C at each time step. The lower boundary of the domain provides a constant heat flux of $F=2$ W/m^2 into the water,

$$S_{bottom} = \frac{F}{\Delta z} \tag{4}$$

where z is the vertical size of the numerical cell. The heat flux at the upper boundary is determined implicitly through Newton's law of heat transfer from the prescribed air temperature T_{air}, the temperature of the surface cell, and the thermal resistance imposed by the thermal conductivity of the surface cell in series with an ice–air heat transfer coefficient of h=15 W/m² K (i.e., windy conditions),

$$S_{top} = \frac{T_{air} - T}{\Delta z} \left[h^{-1} + \frac{\Delta z}{2\bar{k}} \right]^{-1} \tag{5}$$

With only a moderate bottom heat flux F, melt is typically dominated by surface ablation. Surface ablation is treated as follows: each time step the uppermost cell is completely liquid (φ=1) while lower-lying cells still contain ice (φ<1), the ice is made to float up to the surface. This was implemented as a copy cooperation of the porosity and temperature fields "upward" by one cell. Since the thermal conductivity of water is less than the conductivity of ice, the rate of surface ablation may be underestimated.

The development of ice thickness H was calculated from

$$H(t) = \int \varphi(z,t)dz = \sum \varphi(z,t)\Delta z \tag{6}$$

and the maximum ice thickness of the season was used later in the analysis.

The domain was 15 m high with grid size z=0.1 m, initial conditions were φ=1 and T=8 °C on 1 August of each year, and the time step was t=86400 s (1 day), corresponding to the air temperature record. The energy conservation equation was solved implicitly. Since the model did not include melt from solar radiation it was expected that melt rates were underestimated in summer. Simulations were therefore performed separately for each season, i.e. from 1 August until 31 July of the following year. Hence, perennial ice was not able to form.

The time history of ice stress was calculated at each vertical level of the ice growth model. The equations of [11] were used with parameters discussed by [6]. Ice stress was calculated from

$$\frac{d\sigma}{dt} = A\frac{dT}{dt} - B\left(\frac{T_0}{\bar{T}}\right)^m \left(\frac{\sigma}{\sigma_0}\right)^n \tag{7}$$

where σ is the local stress (positive in compression, extension to negative stresses as in [6]), $\bar{T}$ is the average local ice temperature between two time steps, A=E α=200 kPa/K is the product of the relevant linear elastic modulus (cf. [5] for a discussion), E, and linear thermal expansion of the ice, α, B=342 kPa/

day is the product of the elastic modulus and a constant describing creep of ice, $m=1.92$ and $n=3.7$ are fitted constants, and $T_0 = -1\ °C$ and $\sigma_0=100$ kPa are constants for dimensional scaling. The ice temperature record was used to derive input parameters dT/dt and $\overline{T}$, and the non-linear equation was solved implicitly at each time step, i.e. the solution for σ was determined numerically from the value σ^{t-1} one time step t earlier by solving

$$\frac{\sigma - \sigma^{t-1}}{\Delta t} = A\frac{dT}{dt} - B\left(\frac{T_0}{\overline{T}}\right)^m \frac{1}{2}\left[\left(\frac{\sigma}{\sigma_0}\right)^n + \left(\frac{\sigma^{t-1}}{\sigma_0}\right)^n\right]$$

[8]

for σ. The stress σ was set to 0 kPa each time the local temperature was $\geq 0\ °C$, and $\overline{T}$ was not allowed to exceed $-0.001\ °C$ for numerical reasons. A zero-crossing of σ was prevented if the sign of dT/dt rendered this unphysical. Ice fracture in tension or compression was not treated explicitly. Due to the non-linear nature, the calculation of the stress field took significantly more time than the calculation of the temperature field.

At each time step, the line load was calculated from the stress profile according to

$$LL(t) = \int_0^{H(t)} (z,t)dz = \sum(z,t)\Delta z$$

[9]

where LL is the line load at a given time.

For reference, freezing degree days (FDD) were calculated from the seNorge air temperature data according to

$$FDD = -\sum T\Delta t$$

[10]

where T is the daily average temperature or $0\ °C$, whichever is less, and $t = 1$ day.

3.   RESULTS AND DISCUSSION

The data processing procedure is illustrated in Fig. 1 using data of reservoir number 1 (i.e., Tinnsjø in the Telemark region). The air temperature for one season (Fig. 1a) was fed into the model as the sole input, and ice thickness and temperature profiles were calculated based on this (Fig. 1b). From this the maximum ice thickness was determined for the particular season. The development of ice stresses was calculated at each depth of the ice temperature model using ice temperature data of that particular depth (Fig. 1c). Following this, the vertical stress profile was integrated at each time step to yield line load over time (Fig. 1d). The maximum line load of a particular season was determined from

that result. Water temperatures are typically very close to the freezing point in the upper meter of the column (Fig. 1b). Usually, the highest ice loads appear before the ice reached its maximum thickness (in this example, days 195 and 240, respectively) (Figs 1c and 1d).

We verified that modeled ice thickness and peak thermal ice loads are reasonable by comparing model output with five years of measurements in one particular reservoir near Narvik, Norway (Taraldsvikfossen reservoir) [6,12,13]. That reservoir showed peak maximum line loads around 100 kN/m. Since measured loads typically combine effects of thermal loads, water level fluctuations, snow cover and surface flooding, we refrain from a detailed comparison of the data in this study. The general agreement between model and data was anticipated since the stress equations were calibrated to thermal load events in that particular reservoir. Measurements in other regions of Norway do not seem to exist.

Basic metrics of this study, e.g., average ice thickness and average line load, are non-stationary and show a downward trend with time. Fig. 2 exemplifies the trends of the particular reservoir shown in Fig. 1. A downward trend is discernable for both ice thickness and line load. Superimposed on the trend is a considerable inter-annual variability. Since actual thickness and loads depend significantly on the weather of the particular year, expected values will be shown below, i.e. the values along the trend line. For the sake of present-day relevance, reservoir ice loads and thicknesses presented are the values of the respective trend line in 2015/16, labeled as "2010s".

The year-to-year variability around the trend line seen in Fig. 2 is significant compared to the long-term change. Fig. 3 quantifies this by showing the standard deviation (STD) of the detrended maximum lines loads depending on the rate of change of line load for all reservoirs that have >0.1 m maximum ice thickness in the 2010s. The standard deviation (average 38 kN/m) is always greater in magnitude than the rate of change per decade (average -7 kN/m), indicating that it takes several decades for maximum line loads to change consistently (i.e., until what used to be a low maximum line load will be considered a high maximum line load). For example, one may consider a change to be consistent when the expected line load has changed by two standard deviations in a particular reservoir. In this case, the reservoirs that reduced line loads at rates of 15 to 20 kN/m per decade (which have a standard deviation of approximately 50 kN/m) would have seen consistently higher loads 50 to 70 years ago. Applied to the example of the reservoir in Fig. 2, 150 kN/m would have been considered a low maximum line load in the 1950s and 1960s, while 150 kN/m had been at the upper end since the early 2000s.

Fig. 3 shows that there are very few reservoirs that are expected to have seen a slight increase in maximum line loads (<2 kN/m per decade), albeit one that is completely dwarfed by the inter-annual variability.

Fig. 3 indicates the reservoirs that are in the temperate and polar climate groups according to the Köppen climate classification (cf. [14,15] for methodology). Most notably, reservoirs in neither one of these groups show particularly high rates of change or variability. All extremes, i.e. both the greatest and the smallest in both change and variability, are found in reservoirs in the continental climate group. Hence, the Köppen climate groups hold limited predictive power for line load changes and variabilities beyond the realization that neither polar nor temperate regions bear the extremes.

Fig. 4 shows the relationship between expected maximum line load and expected maximum ice thickness in the 2010s. As expected, there is a general tendency for high line loads to be found in thick ice, and the relationship between expected line load and expected ice thickness is approximately linear. While the thinnest ice is found in the temperate climate group, ice in the polar group is not necessarily the thickest and definitely does not show the highest line loads at a given ice thickness.

In an attempt to relate maximum line loads to a quantity that is relatively easy to measure, Fig. 5 shows the expected maximum line load plus one standard deviation in the 2010s versus the expected freezing degree days in the 2010s. One standard deviation above the expected value should not be exceeded in 84% of the years on average, i.e. five out of six years. (Note that Fig.5 shows a correlation of general conditions in the 2010s rather than a correlation valid for individual years.) According to this estimate, locations with less than 500 °C days are expected to see seasonal maximum lines loads rarely exceeding 100 kN/m, while locations with less than 800 °C days will rarely exceed 150 kN/m. With the exception of reservoirs at a few locations, 200 kN/m are expected to be rarely exceeded anywhere in Norway in the 2010s.

The regional distribution of expected maximum line loads in the 2010s across Norway is shown in Fig. 6. The highest line loads are expected in Northern Norway, in particular in the plateaus of Finnmark. Other areas of significant line loads lie in the mountains along the Norwegian-Swedish border and inland in Southern Norway. Reservoirs near the coast and East of the mountains see low to moderate ice loads.

The regional distribution of line load trends differs noticeably from the distribution of loads (Fig. 7). Low rates of ice load reduction are seen in coastal areas that experience low ice loads to begin with. However, the lowest rate of ice load reduction (including slightly increased loads) is seen at high elevation in the mountains of the South-West (in particular Rogaland region), while the highest rate of ice load reduction is found on the East side of those mountains (including the areas around Gudbrandsdalslågen, north of Lillehammer). The low or absent rates of ice load reduction in the South-West could be resulting from weather moving in from the North Sea, possibly in conjunction with a long-term trend of changing storm patterns. However, such climatic links remain to be investigated.
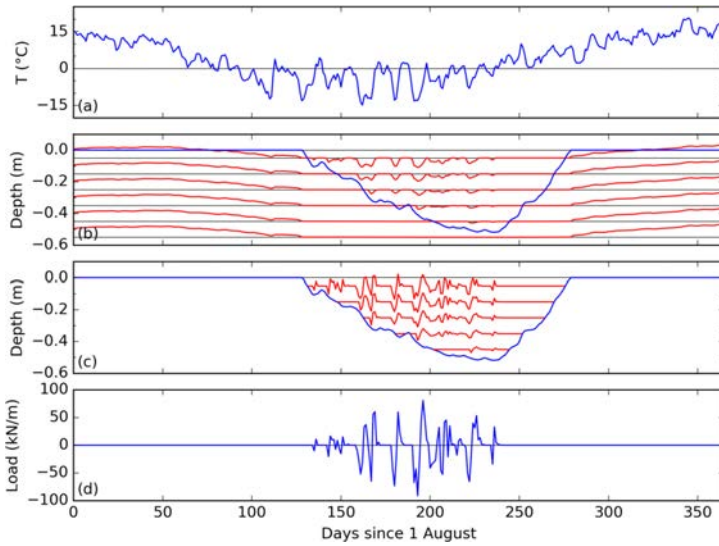
Fig. 1
Example of the data processing pipeline showing (a) air temperature, (b) water/ice temperatures at different depths (no scale, red lines; thin black lines are zero degrees at the respective depth) and ice thickness (blue line), (c) stresses in the ice (red lines, compression is positive) and ice thickness (blue line), and (d) line load. Data used are those of reservoir 1, winter 1998/99.
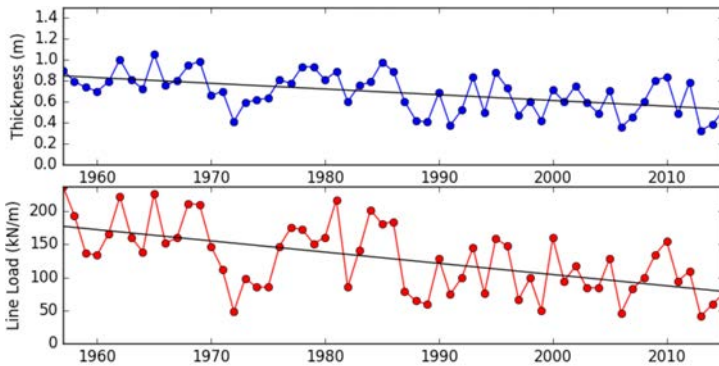

Fig. 2
Example of the development of (a) annual maximum ice thickness with a trend of -0.06 m per decade, and (b) annual maximum line load with a trend of -15 kN/m per decade. Data of reservoir 1.
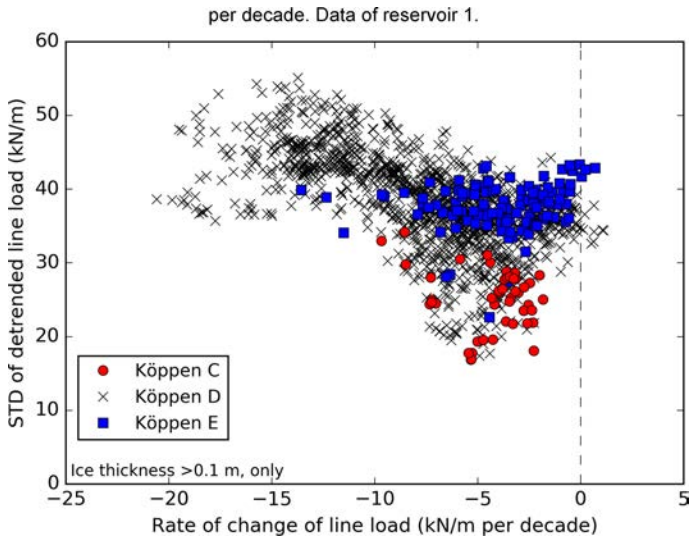
per decade. Data of reservoir 1.

Fig. 3
Standard deviation of detrended line loads versus rate of change of line loads for reservoirs located in Köppen temperate climate (group C, red circles), continental climate (group D, black crosses), and polar climate (group E, blue squares).
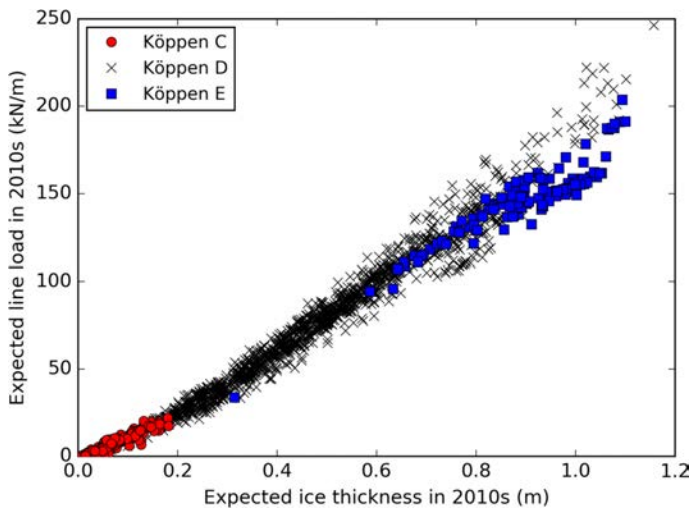

Fig 4.
Expected annual maximum line load vs. expected annual maximum ice thickness in the 2010s for reservoirs located in Köppen temperate climate (group C, red circles), continental climate (group D, black crosses), and polar climate (group E, blue squares).
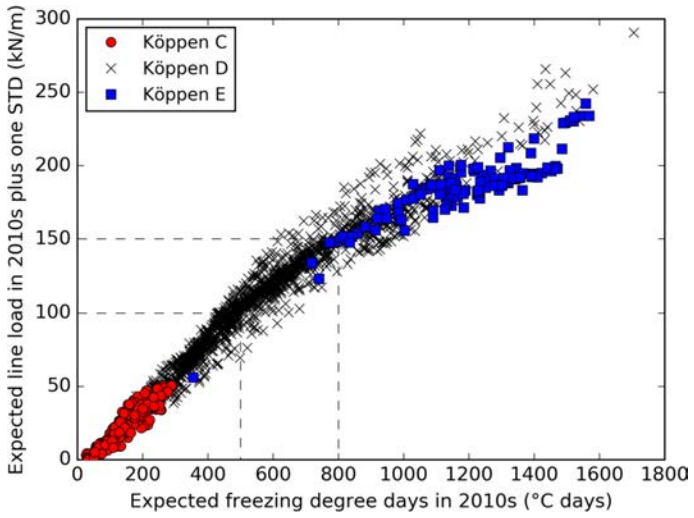
Fig. 5
Rarely exceeded lines loads in the 2010s (i.e., expected line load plus one standard deviation) versus expected freezing degree days.
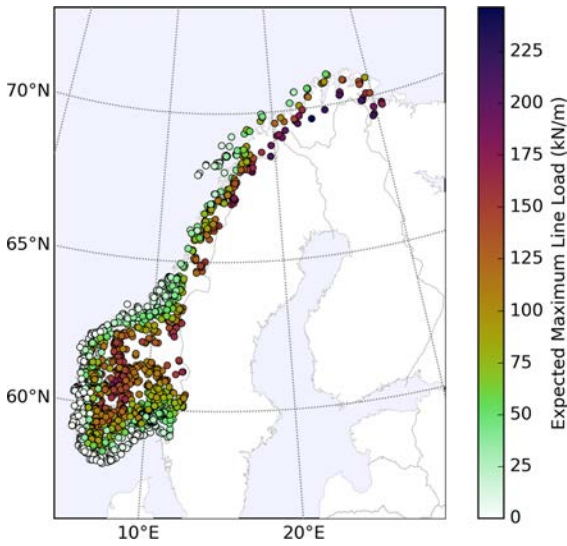

Fig. 6
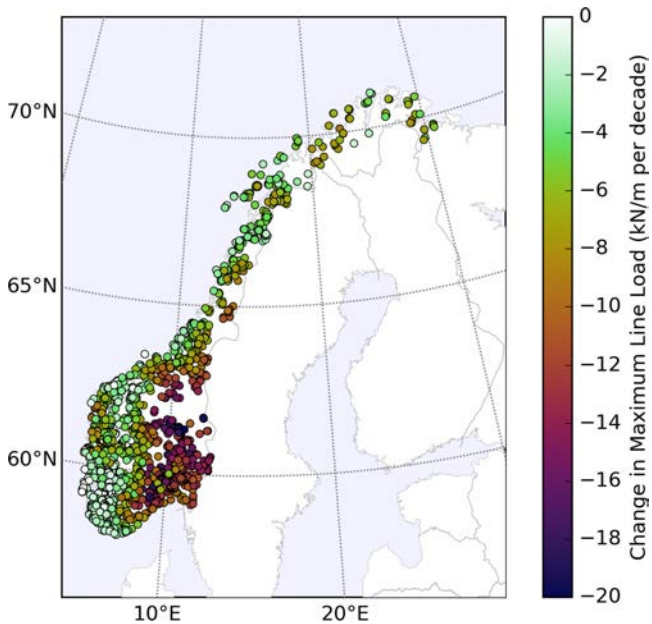Distribution of expected maximum line loads in the 2010s across Norway.

Fig 7.
Regional distribution of line load trends across Norway.

4. CONCLUSION

The presented work gives a first impression of the likely regional and temporal variability of ice loads across Norway. Before the magnitudes presented in this study can be deemed suitable for design a systematic sensitivity study of the model parameters should be conducted, and validation measurements should be conducted in other reservoirs. To-date vertical ice stress profiles have been measured in only one reservoir in Norway. Those measurements showed peak loads around 100 kN/m, and it would be desirable to conduct long-term validation and calibration measurements in reservoirs that are expected to develop thermal loads significantly higher than that.

Line loads were found to differ significantly regionally with inland reservoirs in Northern Norway showing the potential for highest loads. Over the past 60 years, all reservoirs showed a tendency toward decreasing line loads with the notable exception of a few reservoirs in the mountains in the South-West. During this period, a few reservoirs would have seen reductions of their maximum line loads to the extent that their highest potential loads these days used to be their lowest

potential loads 60 years ago. However, trends over a few decades are obscured by inter-annual variability for most reservoirs.

Statistically, regions of generally higher seasonal maximum line loads tend to coincide with regions of generally greater freezing degree days (FDDs). Since FDDs are cheap to calculate they could be used to pre-screen reservoir locations for low ice loads, potentially influencing the selection of design or rehabilitation measures.

The model produces thermal ice loads in hypothetical reservoirs without snow cover, water level fluctuations, ice fracture and surface flooding, and exposed to constant wind conditions, overcast and perpetual darkness. It also assumes identical wind conditions and water depth across all reservoirs. The absence of snow is expected to lead to simulated loads biased high. The assumptions on environmental conditions limit its predictive power for actual ice loads in any particular reservoir and year. However, its ability to calculate inter-annual variability can yield context to ice load measurements. For example, it could be used as a tool to assess whether line loads in a particular year should have been at the high end or at the low end. Hence, the model may be useful to place field measurements of ice loads into a longer-term perspective.

This study shows that static thermal ice loads can be expected to differ significantly regionally in Norway. The long-term trend is toward lower ice loads. The regional dependence of the magnitude of the trend is non-trivial, suggesting that the changing climate has regionally different fingerprints throughout Norway. This should be considered during design and rehabilitation of dams.

ACKNOWLEDGEMENTS

REFERENCES

[1]   Konow, T. and M. Engseth. Evaluering av eksisterende betong- og murdammer (Evaluation of existing concrete and stone dams). *Report 2 – Main Report*. Energi Norge, Norway, 2017, 190 pp.

[2]   Comfort, G., Y. Gong, S. Singh, R. Abdelnour. Static ice loads on dams. *Can. J. Civ. Eng.* 30, 2003, 42–68.

[3]   Sæther, I., Methods for prediction of thermally-induced ice loads on dams and hydro-electrical structures. *Technical Report 2012/03*, Northern Research Institute Narvik, Norway, 2012, 57 pp.

[4]   Gebre, S., K. Alfredsen, L. Lia, M. Stickler, E. Tesaker. Review of ice effects on hydropower systems. *J. Cold Reg. Eng.* 27 (4), 2013, 196–222.

[5]   Cox, G.F.N. A preliminary investigation of thermal ice pressures. *Cold Reg. Sci. Technol.* 9, 1984, 221–229.

[6]   Petrich, C., I. Sæther, L. Fransson, B. Sand, B. Arntsen, Time-dependent spatial distribution of thermal stresses in the ice cover of a small reservoir, *Cold Regions Science and Technology*, 120, 2015, 35-44.

[7]   Côté, A., A. Taras, G. Comfort, and B. Morse. Static ice loads at dam face and at far field. *In Proceedings of the 23rd IAHR International Symposium on Ice*, Michigan, USA, 31 May–3 June 2016, 2016, 8pp.

[8]   Lussana, C., O.E. Tveito, and F. Uboldi. seNorge v2.0: an observational gridded dataset of temperature for Norway. MET report 14-2016, *Norwegian Meteorological Institute, Oslo*, 2016, 108 pp.

[9]   Petrich, C., P.J. Langhorne, Z.F. Sun, Modelling the interrelationships between permeability, effective porosity and total porosity in sea ice, *Cold Regions Science and Technology*, 44(2), 2006, 131-144, https://doi.org/10.1016/j.coldregions.2005.10.001.

[10] Henderson-Sellers, B., New formulation of eddy diffusion thermocline models, *Applied Mathematical Modelling*, 9(6), 1985, 441-446.

[11] Bergdahl, L., and L. Wernersson. Calculated and expected thermal ice pressures in five Swedish lakes. *Report Series B:7*. Chalmers University of Technology, Göteborg, Sweden, 1978, 82 pp.

[12] Petrich, C., I. Sæther, L. Fransson, B. Sand, and B. Arntsen, Preliminary results from two years of ice stress measurements in a small reservoir, *In Proceedings of the 22nd IAHR International Symposium on Ice*, Singapore, 11–15 August 2014, A. W.-K. Law (ed), NEWRI Nanyang Technological University, Singapore. 2014, 452-459.

[13] O'Sadnick, M., C. Petrich, B. Arntsen, and B. Sand, Observations of Ice Stress at Taraldsvikfossen Reservoir, Narvik, Norway. *In Proceedings of the 23rd IAHR International Symposium on Ice*, Ann Arbor, Michigan, USA, 31 May to 3 June 2016. 2016, 10 pp.

[14] Köppen, W., 1884: Die Wärmezonen der Erde, nach der Dauer der heis-sen, gemässigten und kalten Zeit und nach der Wirkung der Wärme auf die organische Welt betrachtet (The thermal zones of the Earth according to the duration of hot, moderate and cold periods and of the impact of heat on the organic world). *Meteorol. Z.*, 1, 215-226.

[15] Kottek, M., J. Grieser, C. Beck, B. Rudolf, and F. Rubel. World Map of the Köppen-Geiger climate classification updated. *Meteorol. Z.*, 15, 2006. 259-263. DOI: 10.1127/0941-2948/2006/0130.